A localized and surprising source of energetic ions in the Uranian magnetosphere between Miranda and Ariel

Ian J. Cohen[1*], Drew L. Turner[1], Peter Kollmann[1], George B. Clark[1], Matthew E. Hill[1], Leonardo H. Regoli[1], and Daniel J. Gershman[2]

[1]Johns Hopkins University Applied Physics Laboratory; Laurel, Maryland, USA.

[2]NASA, Goddard Space Flight Center; Greenbelt, Maryland, USA.

*Corresponding author: Ian Cohen (Ian.Cohen@jhuapl.edu)

Key Points:

- Analysis of Voyager 2 observations revealed a localized source of energetic ions in the region between the moons Miranda and Ariel
- Diffusive transport modeling suggests that typical magnetospheric sources cannot explain the observed characteristics of the energetic ions
- Additional in-situ ion composition and plasma wave observations are necessary to confirm whether these ions are coming from an active moon

Abstract

In situ exploration of Uranus has been limited to a single flyby encounter by the Voyager 2 spacecraft in January 1986. Nonetheless, new investigation has led to significant questions about the origin of energetic ions observed in the region between its moons Miranda and Ariel. Radial and pitch angle diffusion modeling suggests that typical magnetospheric sources cannot explain the observed characteristics of these energetic ions. We suggest that these are likely being introduced by a source from one of these moons and give rise to waves that could result in the observed particle distribution characteristics. This may reveal that internal plasma sources in the system may be important for Uranus' magnetospheric dynamics and may contribute to its unexpectedly strong radiation belts.

Plain Language Summary

Uranus is an oddity in the solar system for a variety of reasons, but mostly as a result of its perpendicular rotation relative to the rest of the planets in the solar system. During its approximately three-day flyby of Uranus in 1986, Voyager 2 captured the only in-situ observations of the planet and its system. New analysis of these three-decade-old observations have revealed a mysterious source of energetic ions in the planet's magnetosphere. These ions were originally explained by dynamics of the system, but new understanding suggests that this is probably unlikely. New simple modeling of the expected behavior of such energetic particles show that sustaining such a population requires a very strong source and specific energization mechanism. Both would potentially be consistent with the ions originating from either Miranda or Ariel. This potentially hints that the Uranian magnetosphere may harbor an ocean world like those known or believed to exist at the other Giant Planets.

1 Introduction

The single glimpse of the Uranus system provided by Voyager 2 revealed surprises and provided observations that have led to new questions (e.g., Paty et al., 2020; Kollmann et al. 2020). Perhaps most significantly, the Voyager 2 flyby revealed that Uranus has an offset and highly-tilted intrinsic magnetic field, with a tilt of ~60º from the rotational axis (Fig. 1) (Paty et al., 2020). Voyager 2 also observed the energetic particle populations at Uranus to be very similar to Earth (Mauk & Fox, 2010), despite the fact that Voyager 2 found much lower densities of plasma in the system than Earth and the Gas Giants (McNutt et al., 1987). Thus, it is unclear from which source plasma the radiation belts could be populated. However, transformational advances in understanding of magnetospheric processes—afforded by observations from missions at several planets in the ensuing decades since the initial analyses of the Voyager 2 observations—provide a new lens through which to reanalyze observations from the Uranian magnetosphere.

The mystery surrounding Voyager 2's discovery of unexpectedly strong radiation belts at Uranus motivated a revisiting of the LECP dataset. This fresh survey revealed a previously underappreciated signature in the energetic particle observations from the Low Energy Charged Particle (LECP) instrument (Krimigis et al., 1977). Specifically, LECP observed a significant (several orders of magnitude) discrepancy between the intensity of energetic particles (both ions and electrons) observed during the outbound leg of the Uranus flyby encounter in the region between Miranda and Ariel compared to the inbound leg (Fig. S1). The Plasma Experiment

(PLS) (Bridge et al., 1977) also reported signatures suggestive of anomalous spacecraft charging in the same region (McNutt et al., 1987).

Such an "asymmetry" in particle fluxes between the inbound and outbound legs of the trajectory may have been expected if the spacecraft encountered these radial distances at very different magnetic latitudes, but that was not the case – the actual difference in magnetic latitude was <20°. While this "asymmetry" was noted in initial analysis of the LECP observations (Mauk et al., 1987), its extreme nature was explained as an artifact of the flyby trajectory because at the time no other solution (e.g., very intense substorm-like injection dynamics) seemed plausible. Fig. S2 shows average PADs observed at three different >300 keV ion energy channels created by using the offset tilted dipole magnetic field model from Ness et al. (1986) to extrapolate the local pitch angle pointing of LECP inbound (24 Jan 1986 17:15-17:30 UT) and outbound (24 Jan 1986 19:45-20:00 UT) to the same magnetic latitude (i.e., ~20° from the outbound leg). Based on this mapping in pitch angle space (using conservation of the first invariant) it was actually determined that because of the differences in magnetic latitude between the inbound and outbound legs of the flyby, the near-90° pitch angle particles seen on the outbound leg could not be seen by Voyager 2 at the higher latitudes on the inbound leg (i.e., they were mirroring at lower latitudes than Voyager 2). It should be emphasized that ion measurements at energies $\lesssim$300 keV are significantly contaminated by penetrating energetic particles (Mauk et al., 1987).

Transient intensity enhancements in both ions (Roussos et al., 2008) and electrons (Roussos et al., 2018) due to events in the solar wind have been observed at other giant planets, but between different orbits. There was also no evidence of drift dispersion and/or extended signatures of such an injection at higher L, both of which might be expected if an injection had occurred sometime during the periapsis pass, as the lack of injection signature on the inbound leg of the trajectory might suggest. Previous work (Cheng et al., 1987) has looked at the LECP energetic particle observations at Uranus and calculated phase space density (PSD) profiles. However, the values of the second adiabatic invariant (K), which they confined their analysis to, restricted the portions of the flyby encounter that they included in their analysis—i.e., L<10 for the inbound leg and L>9 for the outbound leg. The authors concluded that there had to be a source of energetic particles in the inner magnetosphere: specifically, they—like others (Mauk et al., 1987) —suggested substorm-like injections. Further study (Paranicas et al., 1996) focused on the PSD profiles measured by LECP at Uranus, but combined the inbound and outbound legs of the trajectory together, thus averaging out the asymmetry of interest here.

2 Exploring and Confirming the Source

Of particular interest are the pitch angle distributions (PADs) —i.e., the angle of the charged particle velocity vector relative to the background planetary magnetic field vector— measured by LECP, which display extremely steep gradients (Fig. S2). It should be noted that LECP was severely limited in its pitch angle coverage in the region between Miranda and Ariel (see Figure 4 of Mauk et al. (1987)). The nature of these pitch angle (α) distributions is curious. The $\sin^n(\alpha)$ fits (dashed lines) in Fig. 2a show that the n values of the fits get extremely large with n – a paramenter representing the slope in pitch angle space – increased toward higher energies. Such a steep gradient is not due to an enhanced bounce loss cone size, since observations are at a relatively large L-shell (L~7). Maintining such a steep pitch angle gradient, which would be even steeper in terms of equatorial pitch angle, is difficult since any waves— ranging in frequency from ultra-low frequency (ULF) to electromagnetic ion cyclotron

(EMIC)—would act to scatter the particles and isotropize the distribution. In the presence of such waves, this would require a significant and relatively constant source of energetic particles, specifically for those at near-90° pitch angles, at rates that can balance or even overcome any loss/scattering processes from waves. Incidentally, this region between the orbits of Miranda and Ariel was also exactly where Voyager 2 observed intense whistler-mode wave emissions (Kurth & Gurnett, 1991). Maintaining such a steep PAD would require a significant and relatively constant source of energetic particles, specifically for those at near-90° pitch angles, at rates that can balance or even overcome any loss/scattering processes from waves.

To illustrate this point, Figs. 2b-d show results from one-dimensional pitch angle diffusion model simulating the expected evolution of the 1.45-MeV ion (assuming protons) pitch angle distribution observed by LECP at L=6. The model assumes that the inbound and outbound LECP observations place a 6-hour constraint on the evolution of the PAD - i.e., the distribution does not change appreciably over 6 hours. This assumption is supported by additional LECP observations of ions and electrons across the instrument's energy range and the lack of any signatures suggesting a sudden injection. As the initial simulation in Fig. 2b shows, the steep pitch angle gradients observed by Voyager 2 (dashed line) are quickly reduced by pitch angle diffusion over six hours—i.e., approximately the time between the inbound and outbound LECP measurements in the region between Miranda and Ariel. Fig. 2c adds complexity and realism by considering the same pitch angle diffusion scenario but adding rapid (~10-min) losses to the moons at all local pitch angles less than 80º (i.e., those protons that would intersect the moons during a single drift period considering bounce motion along field lines; relative to the Voyager 2 outbound trajectory). As can be seen, this additional loss alongside the ongoing pitch angle diffusion quickly reduces the proton intensity at all α over the 6-hr simulation; while this simulation results in more trapped distributions (i.e., strong peaks centered around $\alpha = 90°$), the proton intensity is reduced by approximately two orders of magnitude compared to what was observed by LECP. While it cannot be ruled out that the inner magnetosphere was serendipitously enhanced during the singular Voyager 2 flyby – i.e., the observed intensities are the final condition of a very slow loss environment instead of the initial condition of a very fast loss environment – it seems incredibly unlikely. Finally, Fig. 2d takes a final step to match diffusion simulations to the observed distributions by adding in a localized, near-90° (i.e., near-equatorial) proton intensity source, which results in a relatively time-stable (i.e., over >6-hr) solution for the 1.45-MeV proton pitch angle distribution that is very similar in magnitude and shape to that observed by LECP. The model uses a pitch angle diffusion coefficient ($D_{\alpha\alpha}$) distribution as a function of α (Fig. S3) and an arbitrarily long (36 hr used here) *e*-folding loss time constant (τ)—approximating slower localized losses due to radial transport and neutral interactions—based on 1-MeV protons in electromagnetic ion cyclotron (EMIC) waves at L = 6 at Earth (e.g., Glauert & Horne, 2005). While it should be noted that this assumption is several orders of magnitude larger than the electron $D_{\alpha\alpha}$ calculated from Voyager 2 observations by Selesnick & Stone (1991), it is still believed to be a reasonable assumption given that previous studies have shown that a distinct temperature anisotropy can lead to enhanced wave growth and that growth mechanisms for EMIC waves are the same for protons as right-handed whistler-mode growth is for electrons (e.g., Usanova et al., 2008, 2012, 2013, and references therein); as previously mentioned, strong whistler-mode wave activity was observed in this region by Voyager 2 (Kurth & Gurnett, 1991); as such, EMIC waves may have been present in this region

as well, but would have been outside the frequency range covered by the Voyager 2 instrumentation.

To assess whether such an energetic particle source is in fact present in the Uranian system, measurements of the phase space density (PSD) profiles of the ions versus L-shell as a function of the first adiabatic invariant (μ) were investigated (Fig. 3) (Green & Kivelson, 2004) using the same LECP response function used by Mauk et al. (1987). These PSD distributions were calculated for local 90° pitch angles, which correspond to approximately K = 0 given the low magnetic latitude. The Voyager 2 trajectory information was processed and converted into several relevant coordinate systems—including the "U1" west-longitude (Ness et al., 1986) and dipole (Mauk et al., 1987) coordinate systems —following the same approach applied in another recent study (DiBraccio & Gershman, 2019). The peak in PSD between 18:00 and 19:00 UT (i.e., planetward of Miranda) cannot be ruled out as a signature resulting only from changes in magnetic latitude and/or moon losses. However, the maximum between Miranda and Ariel at L~7 clearly suggests a source of energetic ions in this region. This peak between Miranda and Ariel is much higher than the PSDs at near the same magnetic latitude (within approximately ±5°) as the other side of those moons and the latitudinal effects expected from μ- and K-conservation are mostly negligible for the <10° latitudinal change at lower latitudes observed here. The clear maximum between Miranda and Ariel at L~7 clearly suggests a source of energetic ions in this region. Similar PSD peaks for protons at Saturn are a common example to illustrate the effect of a local source (e.g., Kollmann et al., 2011, 2017). Other peaks in energetic ion PSD were found just outward of Io at Jupiter (Anglin et al. 1997, Woch et al. 2004), which may serve as an ideal analogy of a geologically-active moon releasing unstable plasma distributions into its environment.

3 Discussion of Potential Sources

It is challenging to definitively determine the source of these energetic particles given the limited—in range, duration, and system coverage—in-situ measurements of the Uranian magnetosphere. In particular, composition measurements of ion species—both mass and charge state—in the suprathermal (10s to 100s keV) energy range are lacking, which could help identify particle sources and acceleration processes. Likewise, field measurements at the relevant frequencies required to assess ion-mode wave processes are missing. However, even the limited measurements obtained at Uranus can be combined with understanding informed by more comprehensive observations in other planetary magnetospheres to assess the feasibility of several sources based on whether they could explain different aspects of the LECP observations—specifically 1) the >300 keV energies, 2) the substantial particle intensities, and 3) the strongly peaked near 90° PADs. Potential energetic particle sources that will be considered here for Uranus are magnetospheric particle injections, cosmic ray albedo neutron decay (CRAND), and sourcing from a moon (i.e., a potentially active moon or sputtering).

"Injections" are sudden enhancements of energetic particles caused by magnetospheric dynamics (e.g., Arnoldy & Chan, 1969; Thomsen, 2013). However, several pieces of observational evidence (or lack thereof) argue against this potential source. First, as previously mentioned, the LECP electron observations display neither any injection-like signature, nor do the injections result in a similarly steep pitch angle gradient. The energy dependence of both the inbound-outbound flux asymmetry and PAD steepness provide further evidence against an

injection source. Additionally, the LECP ion observations show no evidence of drift echoes as might be expected (e.g., Blake et al., 1992) nor any similar injection signatures extended over other L-shells. At Earth, dispersionless injections are most commonly isotropic in pitch angle and extended over a broad range of L-shells (Turner et al., 2017). However, ion distributions at Saturn also exhibit extremely steep PADs, which at low L-shells result from an inflated loss cone and at high L-shells were suggested to be maintained by the CRAND source and the absence of intense EMIC waves (Kollmann et al., 2022). Another potential argument against an injection source is that moon macrosignatures—i.e., longitude averaged depletions of energetic ions at the (minimum) moon L-shells—are observed during both the inbound and outbound legs of the trajectory. Previous work explain that such macrosignatures develop over timescales of moon-particle reencounters, which amount to many drift periods, or days. For example, Paonessa & Cheng (1987) give that the timescale of moon losses at Miranda and Ariel are ~280 hours, or 11-12 days. After such a time scale, any dispersion effect or drift echoes would have disappeared. Though no evidence in the Voyager 2 data nor literature suggests it, there is a possibility that this enhancement may have been a transient radiation belt triggered by a very fortuitously-timed interplanetary coronal mass ejection, as observed at Saturn (e.g., Roussos et al., 2008).

Fig. 4a demonstrates the shape of the PSD profile versus L-shell that would be expected from only inward transport of plasma from the outer magnetosphere (L > 11)—i.e., without any local source in the vicinity of Miranda or Ariel. Note that the modeled PSD values are arbitrary as the model is using simplified, but realistic, physical constraints to simulate the radial shape of the PSD profiles. As can be seen this overall positive slope is very different from the observed PSD shown in Fig. 3, suggesting that some additional source must be playing a role. Fig. 4b shows the expected PSD profile adding a CRAND-like source falling off with distance from the planet (dark blue). CRAND is a well-established and significant source of energetic protons in the radiation belts of Earth and Saturn (e.g., Blake et al., 1992), primarily coming from ring material and planetary atmospheres. This simulation assumes the planet to be the dominant CRAND source in the system and falls off as L^{-2} (e.g., Kollmann et al., 2013); while a contribution from moon CRAND cannot be ruled out, it is considered unlikely. Finally, Fig. 4c shows that the addition of a local source in the region between Miranda and Ariel to the simplified CRAND source results in a PSD profile much closer to that observed by Voyager 2, specifically with the maximum in the region between Miranda and Ariel significantly higher than that inside of Miranda.

The final potential source to be considered is a supply of ions from a moon. Since the 1986 Voyager 2 flyby of Uranus, several moons throughout the solar system have been revealed to be geologically active, often cryo-volcanic, ocean worlds (e.g., Nimmo & Pappalardo, 2016). While debate remains in the Jovian system as to whether Europa may contribute neutrals/ions to the magnetosphere solely from sputtering without the need for active plumes (e.g., Blöcker et al., 2016; Huybrighs et al., 2020; Smyth & Marconi, 2006; Szalay et al., 2022), prior work in the Saturn system found it difficult to make sense of the observed plasma distributions before Encealadus was discovered to be an ocean world (e.g., Burger et al. 2007; Jurac et al., 2002; Jurac & Richardson, 2005; Shi et al., 1995). While sputtering from the surface cannot be ruled out, the conclusions made here are consistent with either or both of Miranda and/or Ariel being

an ocean world, as has been recently suggested (e.g., Hendrix et al., 2019; Ćuk et al., 2020; Schenk & Moore, 2020; Cartwright et al., 2021; Beddingfield et al., 2022a,b).

It must be emphasized that the narrow pitch angle source required to obtain the results in Fig. 2d matches that expected from newly-created pickup ions (Coates & Jones, 2009). Specifically, for the Uranian system, this effect is enhanced by the fact that the electric field magnitude, responsible for giving the initial acceleration to the pickup ions, is strongest when the source is located at the magnetic equator (Cochrane et al., 2021). These effects combined contribute to the highly localized and narrow pitch angle nature of the expected source. As previously mentioned, the introduction of a preferentially trapped population of thermal and/or suprathermal plasma from either sputtering from the surface or an active moon and this pickup ionization process could be expected to generate a significant temperature anisotropy that would drive wave growth that is expected to result in high intensities of both the observed whistler-mode waves (e.g., Kurth & Gurnett, 1991) as well as EMIC waves (unobservable by Voyager 2) that could potentially accelerate the newly-sourced thermal or suprathermal population up to the >1 MeV energies observed by Voyager 2 via strong drift- and/or gyro-resonance, which would isotropize the lower-energy source population while contributing to the very trapped energetic particle population. For example, with gyro-resonant acceleration in quasi-linear diffusion theory, accelerated particles are preferentially accelerated at higher energies and diffuse towards 90° equatorial PA (e.g., Horne et al., 2005, and references therein) by waves generated by strong anisotropies in the lower-energy, suprathermal particles of the same species.

In either case, the location of the maximum in the PSD profiles at L~6 (Fig. 4) makes it unclear which of these two moons may be the most likely potential source, since such PSD values usually fall off closer to the planet (evidence for Ariel) but moon material also tends to move outwards (evidence for Miranda). An expected source from either moon could be estimated using the source required to sustain the pitch angle distributions shown in the simple diffusion model shown in Fig. 2d (see Supplementary Material). Other Voyager 2 observations provide potential further evidence to support the case for a moon source. Unfortunately, at Uranus, the LECP instrument could not measure ion composition below ~500 keV/nuc (Mauk et al., 1987)—e.g., 2 MeV for helium, 8 MeV for oxygen; thus, it is unsurprising that LECP did not see any non-proton populations that may have been sourced by an active Uranian moon as it was unlikely that these species were easily energized to such extreme energies; however, evidence exists that such heavy ions can be accelerated to suprathermal energies by EMIC waves (Wang et al., 2019). Additional measurements from PLS suggest that there are heavier ions in the region between Miranda and Ariel (McNutt et al., 1987). Similarly, the aforementioned PLS signatures of anomalous spacecraft charging could possibly be a result of flying through a dense torus or cloud of ionized particles, including salts (Behannon et al., 1977).

4 Conclusions

New analysis of the LECP obserbations from the Voyager 2 flyby of the Uranus system have revealed a surprisingly intense source of energetic ions in the region between the moons Miranda and Ariel. Consideration of the unique pitch angle distribtutions observed in this population has resulted in the conclusion that the observed energetic ions are most likely originating from cold neutral particles coming from one of the nearby moons – i.e., Miranda or Ariel. The leading hypothesis is that one or both of the moons source low-energy neutrals into

the magnetosphere via sputtering or an active subsurface ocean. This population is then ionized and energized by wave-particle interactions driven by anisotropies driven in the origination of the plasma itself or by the influence of secondary processes like pickup ionization. Ultimately, the accelerating wave-particle interaction processes sculpt the observed preferentially-trapped energetic ion population. However, further investigation of this mysterious energetic ion PAD will require additional observations from the Uranian system, preferably from an orbiter mission that is equipped with instruments to measure the thermal plasma properties and composition, suprathermal (tens to hundreds of keV) ion composition, with both mass and charge-state, and wave activity extending into the ion-cyclotron modes (i.e., EMIC waves).

Acknowledgments

The authors would like to thank Barry Mauk, Ralph McNutt, Tom Krimigis, and Doug Hamilton for extremely helpful insight and expertise in interpreting the Voyager 2 instruments and measurements. We would also like to thank Alexander Drozdov for useful discussions on diffusion processes. This research was funded by the NASA Voyager Interstellar Mission (NASA contract NNN06AA01C) and NASA grant 80NSSC21K1040.

Open Research

The data utilized in this study was obtained from the NASA Planetary Data System (PDS) Planetary Plasma Interactions Node. The respective files can be found at: https://doi.org/10.17189/1520024 (LECP energy distribution), https://doi.org/10.17189/1520025 (LECP pitch angle information), https://doi.org/10.17189/1520034 (MAG), and https://doi.org/10.17189/1520040 (spacecraft position). The processed data, related code, and simulations used in the analysis are available at https://doi.org/10.5281/zenodo.7308665.

References

Anglin, J. D., Burrows, J. R., Mu, J. L., and Wilson, M. D. (1997), Trapped energetic ions in Jupiter's inner magnetosphere, *J. Geophys. Res*., *102*(A1), 1– 36, doi:10.1029/96JA02681.

Arnoldy, R. L., and Chan, K. W. (1969), Particle substorms observed at the geostationary orbit, J. Geophys. Res., 74(21), 5019– 5028, doi:10.1029/JA074i021p05019.

Bagenal, F. (2013), Planetary Magnetospheres, in *Planets, Stars and Stellar Systems. Volume 3: Solar and Stellar Planetary Systems* (eds. T. D. Oswalt, L. French, P. Kalas), doi:10.1007/978-94-007-5606-9_6.

Beddingfield, C. B., R. J. Cartwright, E. Leonard, T. Nordheim, and F. Scipioni (2022a), Ariel's Elastic Thicknesses and Heat Fluxes, *PSJ*, 3, 106, doi:10.3847/PSJ/ac63d1.

Beddingfield, C. B., E. Leonard, R. J. Cartwright, C. Elder, and T. A. Nordheim (2022b), High Heat Flux near Miranda's Inverness Corona Consistent with a Geologically Recent Heating Event, *PSJ*, 3, 174, doi10.3847/PSJ/ac7be5.

Behannon, K.W., Acuna, M.H., Burlaga, L.F. et al. Magnetic field experiment for Voyagers 1 and 2. Space Sci Rev 21, 235–257 (1977). https://doi.org/10.1007/BF00211541

Blake, J. B., W. A. Kolasinski, R. W. Fillius, and E. G. Mullen (1992), Injection of electrons and protons with energies of tens of MeV into L < 3 on 24 March 1991, Geophys. Res. Lett., 19(8), 21-824, https://doi.org/10.1029/92GL00624.

Blöcker, A., Saur, J., and Roth, L. (2016), Europa's plasma interaction with an inhomogeneous atmosphere: Development of Alfvén winglets within the Alfvén wings, *J. Geophys. Res. Space Physics*, 121, 9794– 9828, doi:10.1002/2016JA022479.

Bridge, H.S., Belcher, J.W., Butler, R.J. et al. The plasma experiment on the 1977 Voyager Mission. Space Sci Rev 21, 259–287 (1977). https://doi.org/10.1007/BF00211542

320 Burger, M. H., Sittler, E. C., Johnson, R. E., Smith, H. T., Tucker, O. J., and Shematovich, V.
321 I. (2007), Understanding the escape of water from Enceladus, *J. Geophys. Res.*, 112, A06219,
322 doi:10.1029/2006JA012086.
323 Cheng, A. F., Krimigis, S. M., Mauk, B. H., Keath, E. P., Maclennan, C. G., Lanzerotti, L. J.,
324 Paonessa, M. T., and Armstrong, T. P. (1987), Energetic ion and electron phase space
325 densities in the magnetosphere of Uranus, J. Geophys. Res., 92(A13), 15315– 15328,
326 doi:10.1029/JA092iA13p15315.
327 Coates, A. J. and G. H. Jones (2009), Plasma environment of Jupiter family comets, Planetary
328 and Space Science, Volume 57, Issue 10, 1175-1191,
329 https://doi.org/10.1016/j.pss.2009.04.009.
330 Cochrane, C. J., Vance, S. D., Nordheim, T. A., Styczinski, M. J., Masters, A., & Regoli, L. H.
331 (2021). In search of subsurface oceans within the Uranian moons. Journal of Geophysical
332 Research: Planets, 126, e2021JE006956. https://doi.org/10.1029/2021JE006956
333 Ćuk, M., M. El Moutamid, and M. S. Tiscareno (2020), Dynamical History of the Uranian
334 System, PSJ, 1, 22, doi: 10.3847/PSJ/ab9748.
335 DiBraccio, G. A., & Gershman, D. J. (2019). Voyager 2 Constraints on Plasmoid-Based
336 Transport at Uranus. Geophysical Research Letters, 46, 10710– 10718.
337 https://doi.org/10.1029/2019GL083909
338 Dougherty et al. (2006), Identification of a Dynamic Atmosphere at Enceladus with the Cassini
339 Magnetometer, Science, 311, 5766, 1406-1409,
340 https://www.science.org/doi/10.1126/science.1120985.

Glauert, S. A., and Horne, R. B. (2005), Calculation of pitch angle and energy diffusion coefficients with the PADIE code, *J. Geophys. Res.*, *110*, A04206, doi:10.1029/2004JA010851.

Green, J. C., and Kivelson, M. G. (2004), Relativistic electrons in the outer radiation belt: Differentiating between acceleration mechanisms, J. Geophys. Res., 109, A03213, doi:10.1029/2003JA010153.

Hendrix, A. R., T. A. Hurford, L. M. Barge, M. T. Bland, J. S. Bowman, W. Brinckerhoff, B. J. Buratti, M. L. Cable, J. Castillo-Rogez, G. C. Collins, S. Diniega, C. R. German, A. G. Hayes, T. Hoehler, S. Hosseini, C. J.A. Howett, A. S. McEwen, C. D. Neish, M. Neveu, T. A. Nordheim, G. W. Patterson, D. A. Patthoff, C. Phillips, A. Rhoden, B. E. Schmidt, K. N. Singer, J. M. Soderblom, and S. D. Vance (2019), The NASA Roadmap to Ocean Worlds, *Astrobiology*, 19, 1, 1-144, doi:10.1089/ast.2018.1955.

Horne, R. B., Thorne, R. M., Glauert, S. A., Albert, J. M., Meredith, N. P., and Anderson, R. R. (2005), Timescale for radiation belt electron acceleration by whistler mode chorus waves, *J. Geophys. Res.*, 110, A03225, doi:10.1029/2004JA010811.

Huybrighs, H. L. F., Roussos, E., Blöcker, A., Krupp, N., Futaana, Y., Barabash, S., et al. (2020). An active plume eruption on Europa during Galileo flyby E26 as indicated by energetic proton depletions. *Geophysical Research Letters*, 47, e2020GL087806. https://doi.org/10.1029/2020GL087806

Jurac, S., McGrath, M. A., Johnson, R. E., Richardson, J. D., Vasyliunas, V. M., and Eviatar, A., Saturn: Search for a missing water source, *Geophys. Res. Lett.*, 29(24), 2172, doi:10.1029/2002GL015855, 2002.

Jurac, S., and Richardson, J. D. (2005), A self-consistent model of plasma and neutrals at Saturn: Neutral cloud morphology, *J. Geophys. Res.*, 110, A09220, doi:10.1029/2004JA010635.

Kohlhase, C.E., Penzo, P.A. Voyager mission description. Space Sci Rev 21, 77–101 (1977). https://doi.org/10.1007/BF00200846

Kollmann, P., Cohen, I., Allen, R.C. et al. Magnetospheric Studies: A Requirement for Addressing Interdisciplinary Mysteries in the Ice Giant Systems. Space Sci Rev 216, 78 (2020). https://doi.org/10.1007/s11214-020-00696-5

Kollmann, P., E. Roussos, G. Clark, J. F. Cooper, S. J. Sturner, A. Kotova, L. Regoli, Y. Y. Shprits, N. Aseev, and N. Krupp (2022), Spectra of Saturn's proton belts revealed, Icarus, 376, 114795, https://doi.org/10.1016/j.icarus.2021.114795.

Kollmann, P., E. Roussos, C. Paranicas, N. Krupp, and D. K. Haggerty (2013), Processes forming and sustaining Saturn's proton radiation belts, *Icarus, 222*, 323-341, doi: 10.1016/j.icarus.2012.10.033.

Krimigis, S. M., Armstrong, T. P., Axford, W. I., Cheng, A. F., Gloeckler, G., Hamilton, D. C., Keath, E. P., Lanzerotti, L. J., and Mauk, B. H. (1986), The Magnetosphere of Uranus: Hot Plasma and Radiation Environment, Science, 233, 4759, 97-102, https://www.science.org/doi/10.1126/science.233.4759.97.

Krimigis, S.M., Armstrong, T.P., Axford, W.I. et al. The Low Energy Charged Particle (LECP) experiment on the Voyager spacecraft. Space Sci Rev 21, 329–354 (1977). https://doi.org/10.1007/BF00211545

Kurth, W. S., and Gurnett, D. A. (1991), Plasma waves in planetary magnetospheres, J. Geophys. Res., 96(S01), 18977– 18991, doi:10.1029/91JA01819.

Mauk, B. H., and Fox, N. J. (2010), Electron radiation belts of the solar system, J. Geophys. Res., 115, A12220, doi:10.1029/2010JA015660.

Mauk, B. H., Krimigis, S. M., Keath, E. P., Cheng, A. F., Armstrong, T. P., Lanzerotti, L. J., Gloeckler, G., and Hamilton, D. C. (1987), The hot plasma and radiation environment of the Uranian magnetosphere, J. Geophys. Res., 92(A13), 15283– 15308, doi:10.1029/JA092iA13p15283.

McNutt, R. L., Selesnick, R. S., and Richardson, J. D. (1987), Low-energy plasma observations in the magnetosphere of Uranus, J. Geophys. Res., 92(A5), 4399– 4410, doi:10.1029/JA092iA05p04399.

Ness, N. F., Acuna, M. H., Behannon, K. W., Burlaga, L. F., Connerney, J. E. P., Lepping, R. P., and Neubauer, Fritz M. (1986), Magnetic Fields at Uranus, *Science*, 233, 4759, pp. 85-89, https://www.science.org/doi/10.1126/science.233.4759.85.

Nimmo, F., and Pappalardo, R. T. (2016), Ocean worlds in the outer solar system, J. Geophys. Res. Planets, 121, 1378– 1399, doi:10.1002/2016JE005081.

Paonessa, M. T., and Cheng, A. F. (1987), Satellite sweeping in offset, tilted dipole fields, J. Geophys. Res., 92(A2), 1160– 1166, doi:10.1029/JA092iA02p01160.

Paranicas, C., Cheng, A. F., and Mauk, B. H. (1996), Charged particle phase space densities in the magnetospheres of Uranus and Neptune, J. Geophys. Res., 101(A5), 10681– 10693, doi:10.1029/96JA00077.

Paty, Carol, Arridge, Chris S., Cohen, Ian J., DiBraccio, Gina A., Ebert, Robert W. and Rymer, Abigail M. (2020)m Ice giant magnetospheres, Phil. Trans. R. Soc. A., 3782019048020190480 http://doi.org/10.1098/rsta.2019.0480

Roussos et al. (2018), Drift-resonant, relativistic electron acceleration at the outer planets: Insights from the response of Saturn's radiation belts to magnetospheric storms, Icarus, 305, 160-173, https://doi.org/10.1016/j.icarus.2018.01.016.

Roussos, E., Krupp, N., Armstrong, T. P., Paranicas, C., Mitchell, D. G., Krimigis, S. M., Jones, G. H., Dialynas, K., Sergis, N., and Hamilton, D. C. (2008), Discovery of a transient radiation belt at Saturn, Geophys. Res. Lett., 35, L22106, doi:10.1029/2008GL035767.

Schenk, P. M. and J. M. Moore (2020), Topography and geology of Uranian mid-sized icy satellites in comparison with Saturnian and Plutonian satellites, *Phil. Trans. R. Soc. A.*, **378,** 2020010220200102, doi:10.1098/rsta.2020.0102.

Selesnick, R. S., and Stone, E. C. (1991), Energetic electrons at Uranus: Bimodal diffusion in a satellite limited radiation belt, *J. Geophys. Res.*, *96*(A4), 5651– 5665, doi:10.1029/90JA02696.

Shi, M., Baragiola, R. A., Grosjean, D. E., Johnson, R. E., Jurac, S., and Schou, J. (1995), Sputtering of water ice surfaces and the production of extended neutral atmospheres, *J. Geophys. Res.*, 100(E12), 26387– 26395, doi:10.1029/95JE03099.

Sittler, E. C., Ogilvie, K. W., and Selesnick, R. (1987), Survey of electrons in the Uranian magnetosphere: Voyager 2 observations, J. Geophys. Res., 92(A13), 15263– 15281, doi:10.1029/JA092iA13p15263.

Smith, H. T., Johnson, R. E., Perry, M. E., Mitchell, D. G., McNutt, R. L., and Young, D. T. (2010), Enceladus plume variability and the neutral gas densities in Saturn's magnetosphere, J. Geophys. Res., 115, A10252, doi:10.1029/2009JA015184.

Smyth, W. H. & M. L. Marconi (2006), Europa's atmosphere, gas tori, and magnetospheric implications, *Icarus*, *181*, 2, 510-526, doi: 0.1016/j.icarus.2005.10.019.

Stone, E. C. and E. D. Miner (1986), The voyager 2 encounter with the uranian system, Science, 233(4759), 39-43, doi:10.1126/science.233.4759.39.

Szalay, J. R., Smith, H. T., Zirnstein, E. J., McComas, D. J., Begley, L. J., Bagenal, F., et al. (2022). Water-group pickup ions from Europa-genic neutrals orbiting Jupiter. *Geophysical Research Letters*, 49, e2022GL098111. https://doi.org/10.1029/2022GL098111

Thomsen, M. F. (2013), Satur''s magnetospheric dynamics, Geophys. Res. Lett., 40, 5337– 5344, doi:10.1002/2013GL057967.

Turner, D. L., Fennell, J. F., Blake, J. B., Claudepierre, S. G., Clemmons, J. H., Jaynes, A. N., … Reeves, G. D. (2017). Multipoint observations of energetic particle injections and substorm activity during a conjunction between Magnetospheric Multiscale (MMS) and Van Allen Probes. Journal of Geophysical Research: Space Physics, 122, 11,481– 11,504. https://doi.org/10.1002/2017JA024554

Usanova, M. E., F. Darrouzet, I. R. Mann, and J. Bortnik (2013), Statistical analysis of EMIC waves in plasmaspheric plumes from Cluster observations, *J. Geophys. Res. Space Physics*, *118*, doi:10.1002/jgra.50464.

Usanova, M. E., I. R. Mann, J. Bortnik, L. Shao, and V. Angelopoulos (2012), THEMIS observations of electromagnetic ion cyclotron wave occurrence: Dependence on AE, SYMH, and solar wind dynamic pressure, *J. Geophys. Res*., *117*, A10218, doi:10.1029/2012JA018049.

Usanova, M. E., I. R. Mann, I. J. Rae, Z. C. Kale, V. Angelopoulos, J. W. Bonnell, K.-H. Glassmeier, H. U. Auster, and H. J. Singer (2008), Multipoint observations of magnetospheric compression-related EMIC Pc1 waves by THEMIS and CARISMA, *Geophys. Res. Lett*., *35*, L17S25, doi:10.1029/2008GL034458.

453 Wakeford H. R. and Dalba P. A. 2020The exoplanet perspective on future ice giant exploration,
454 Phil. Trans. R. Soc. A.3782020005420200054 http://doi.org/10.1098/rsta.2020.0054
455 Wang, Z., K. Sun, Y. Zhang, and H. Zhai (2019), Heavy ion acceleration by EMIC waves in the
456 near-Earth plasma sheet, Phys. Plasmas, 26, 022903, https://doi.org/10.1063/1.5075509.
457 Woch, J., N. Krupp, A. Lagg, and A. Tomás (2004), The structure and dynamics of the Jovian
458 energetic particle distribution, *Adv. Space Res*., *33*, 11, 2030-2038, doi:
459 10.1016/j.asr.2003.04.050.
460

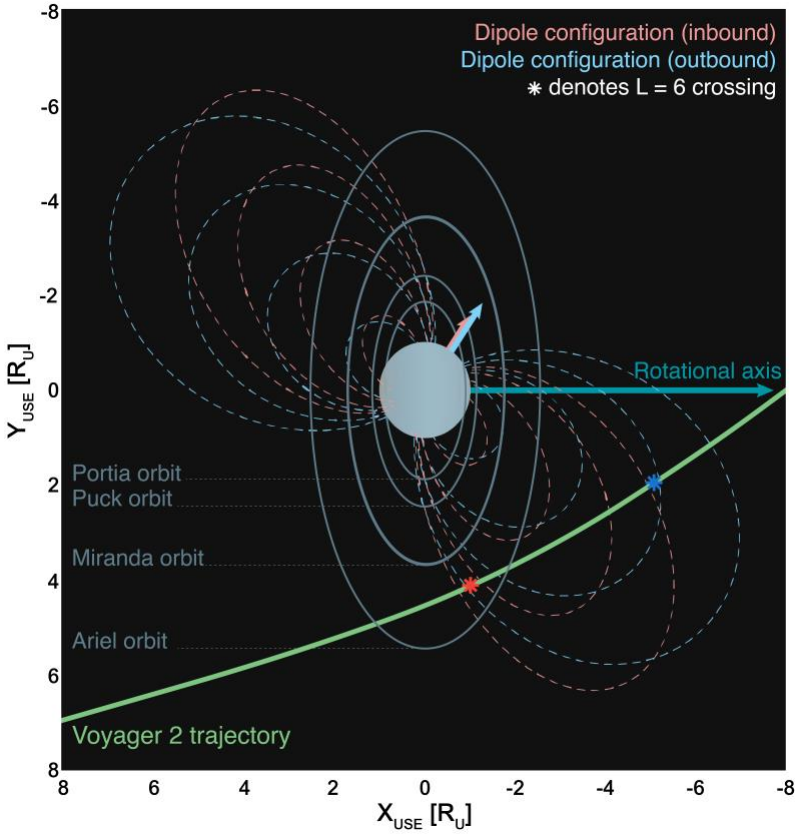

461 **Fig. 1.** Simulation of the 1986 Voyager 2 flyby encounter of Uranus. The complexity and
462 dynamics of the Uranian magnetosphere are demonstrated by the variation in magnetic
463 configuration between the inbound orbit (red) and outbound orbit (blue). Dipolar magnetic field
464 lines at L-shells of 2, 4, 6, and 8 are shown for each configuration.

465

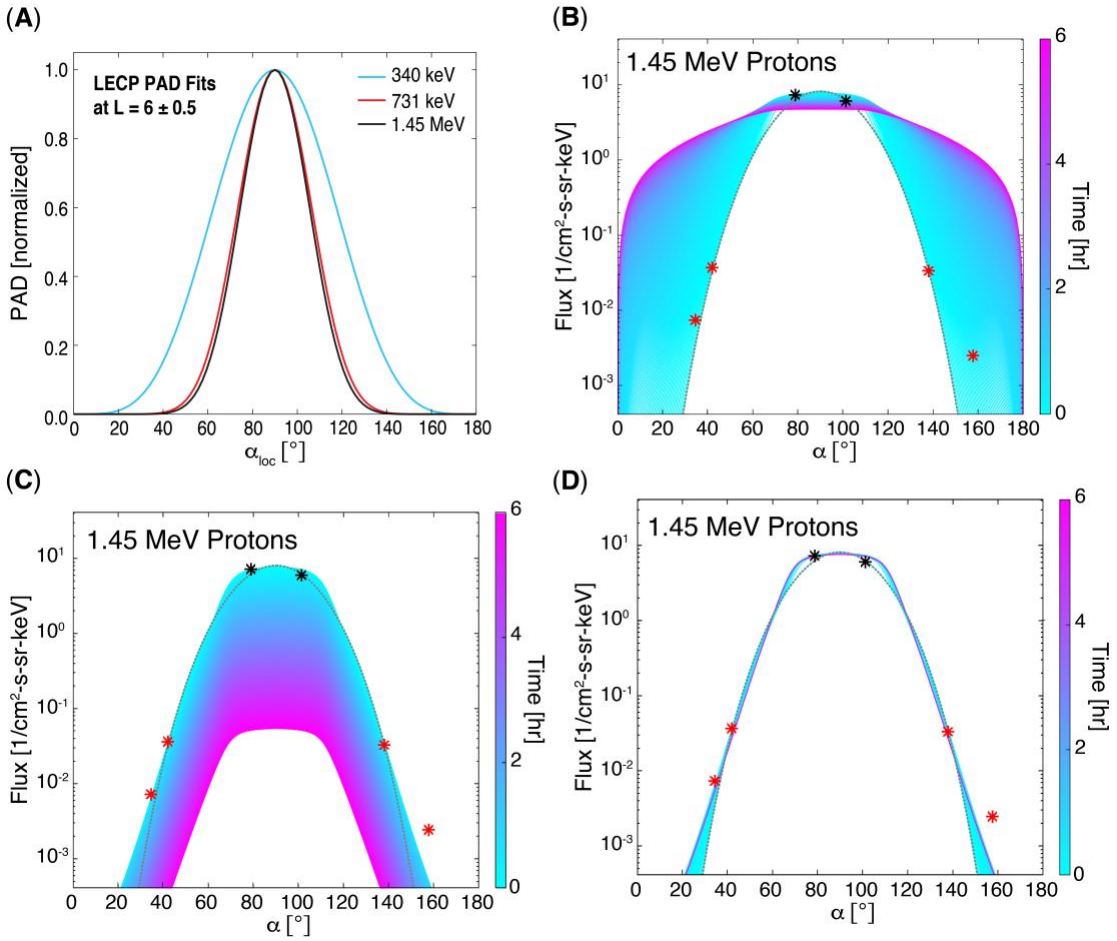

Fig. 2. Simple one-dimensional pitch angle diffusion modeling suggests that an energetic particle source is required to sustain the steep pitch angle gradients observed by LECP. (A) Comparison of $\sin^n(\alpha)$ fit for the average PADs at three different >300 keV ion energy channels created by mapping ions at L = 6 ± 0.5 from both the inbound (red; 24 Jan 1986 17:15-17:30 UT) and outbound (black; 24 Jan 1986 19:45-20:00 UT) legs of the flyby trajectory to the local pitch angle and combining them with the local pitch angle for the outbound trajectory using conservation of the first adiabatic invariant, μ. (B) The expected evolution of the 1.5-MeV ion (assuming protons) pitch angle distribution observed by LECP at L=6 assuming an Earth-like pitch angle diffusion coefficient ($D_{\alpha\alpha}$). (C) The same scenario but adding losses to the moons at all local pitch angles <80° on a 10-min loss timescale. (D) Adding a Gaussian pitch angle source centered at α = 90° with σ = 1.5° and an amplitude of $S_0 = 1.26\times10^{11}$ cm^{-2}-s^{-1}-sr^{-1}-MeV^{-1}/s. This

477 analysis shows that pitch angle diffusion would eliminate the observed steep pitch angle
478 gradients unless a very narrow source is present.
479

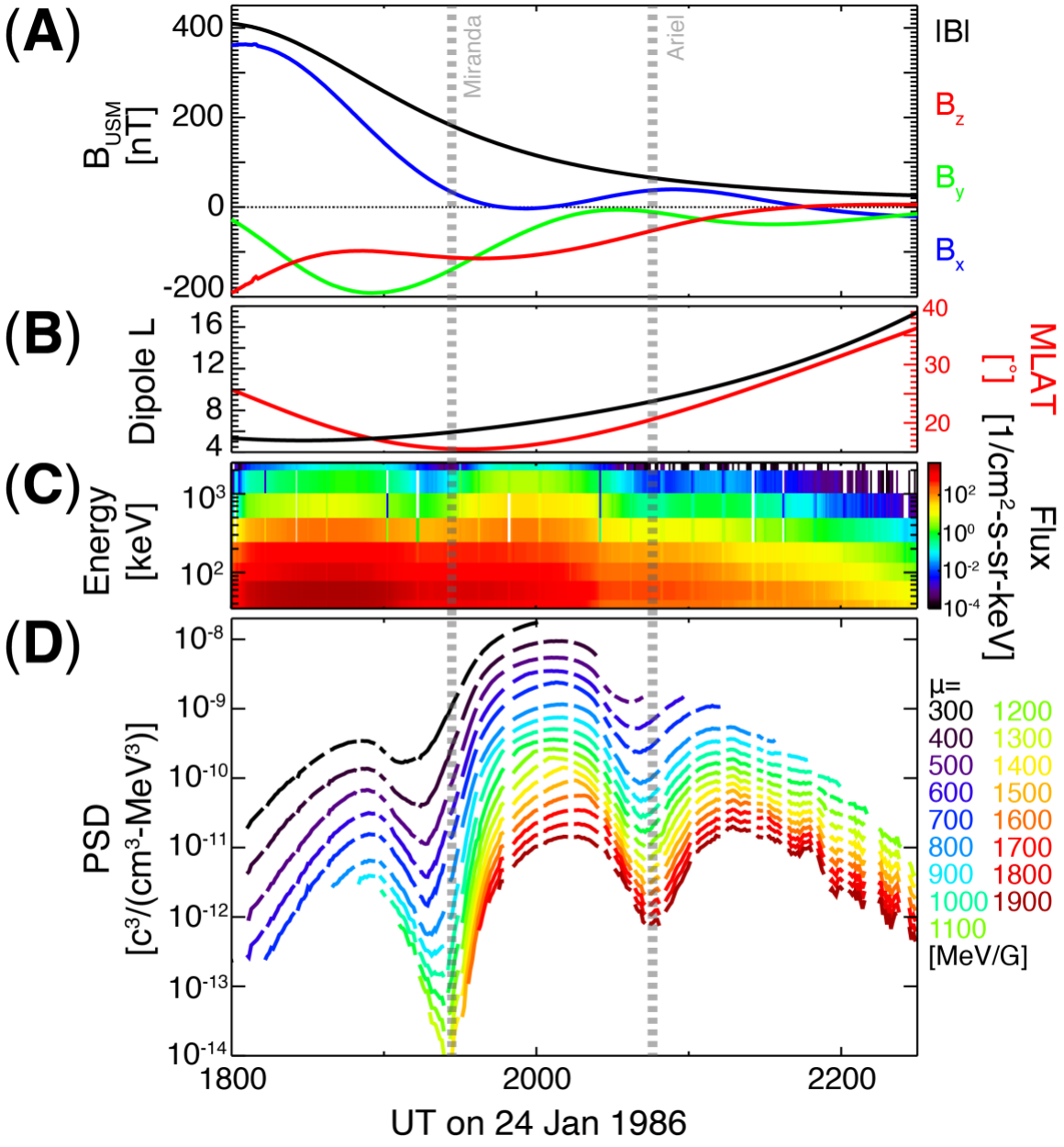

Fig. 3. New phase space density analysis clearly indicates a source of energetic ions in the region between Miranda and Ariel. (A) The observed magnetic field from the Voyager 2 magnetometer [34]. (B) The dipole-L calculated using the offset tilted dipole model from (Ness et al., 1986). (C) The ion flux observed by the LECP instrument (Krimigis et al., 1977). (D) The calculated PSD profiles determined using the LECP and MAG observations versus time for several values

of constant the first adiabatic invariant (μ). The minima surrounding the moons Miranda and Ariel are due to energetic particle losses from interactions with the moons (e.g., Paonessa & Cheng, 1987). However, the very clear maximum between Miranda and Ariel at L~7 clearly suggests a source of energetic ions in this region.

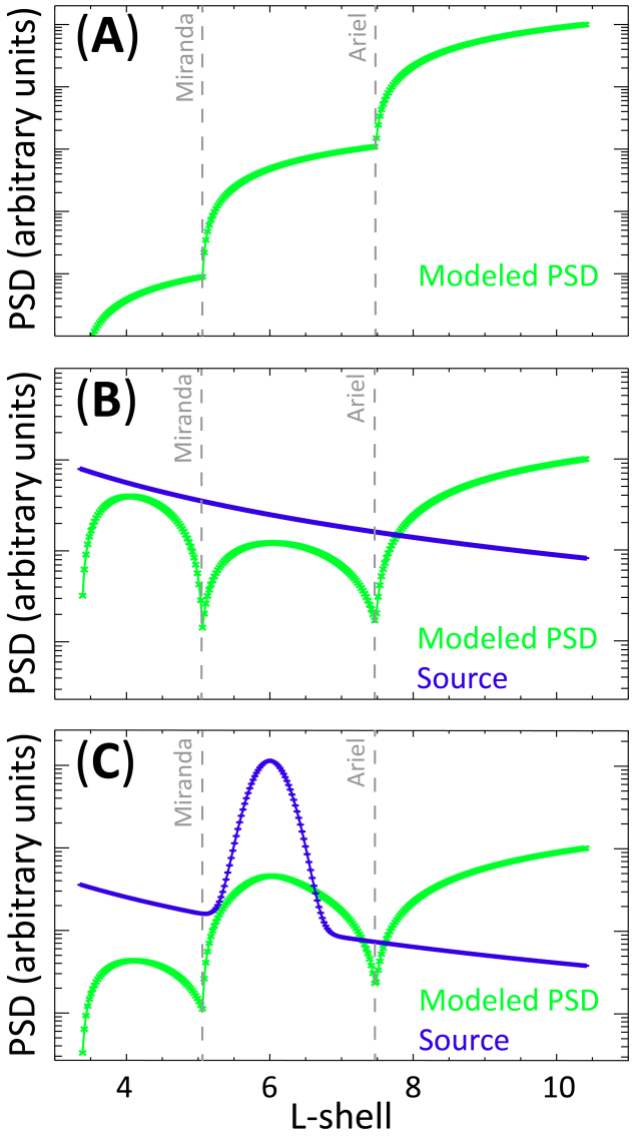

Fig. 4. Modeling of the expected radial distribution of ion phase space density shows that the observed global maximum between Miranda and Ariel requires a significant local source. (A) The expected PSD profile versus L-shell expected from only inward transport of plasma from the outer magnetosphere (L > 11), combined with absorption at the moon orbits. (B) The profile assuming a CRAND-like source falling off with distance from the planet (dark blue). (C) The profile adding a local source in the region between Miranda and Ariel to the simplified CRAND source.